Mediterranean Marine Science

Vol 23, No 3 (2022)

VOL 23, No 3 (2022)

Variability of early autumn planktonic assemblages in the strait of Gibraltar: a regionalization analysis

NEREA VALCÁRCEL-PÉREZ, EDUARDO RAMÍREZ-ROMERO, CARLOS M. GARCÍA, JUAN IGNACIO GONZÁLEZ-GORDILLO, FIDEL ECHEVARRÍA

doi: 10.12681/mms.27623

Research Article

Mediterranean Marine Science
Indexed in WoS (Web of Science, ISI Thomson) and SCOPUS
The journal is available on line at http://www.medit-mar-sc.net
www.hcmr.gr
DOI: http://doi.org/10.12681/mms.27623

Variability of early autumn planktonic assemblages in the strait of Gibraltar: a regionalization analysis

Nerea VALCÁRCEL-PÉREZ[1], Eduardo RAMÍREZ-ROMERO[2], Carlos M. GARCÍA[3,4], Juan Ignacio GONZÁLEZ-GORDILLO[3,4] and Fidel ECHEVARRÍA[3,4]

[1] Málaga Oceanographic Centre. IEO, CSIC. Puerto Pesquero s/n, 29640 Fuengirola, Málaga, Spain
[2] Institute of Marine Sciences of Andalusia, ICMAN-CSIC, Puerto Real, 11510, Cádiz, Spain
[3] Department of Biology, University of Cádiz. Campus Río San Pedro SN. Puerto Real, Cádiz, 11510, Spain
[4] Marine Research Institute (INMAR), International Campus of Excellence in Marine Science (CEI-MAR), University of Cádiz, Puerto Real, 11510 Cádiz, Spain

Corresponding author: Nerea Valcárcel-Pérez; nerea.valcarcel@ieo.csic.es

Contributing Editor: Soultana ZERVOUDAKI

Received: 26 June 2021; Accepted: 31 May 2022; Published online: 29 July 2022

Abstract

The Strait of Gibraltar (SG) is the only connection of the Mediterranean Sea with the global circulation. The SG is an outstanding marine region to explore physical-biological coupling of pelagic communities due to its hydrodynamic complexity, including strong tidal forcing and marked spatial gradients and fronts. The authors have unravelled the role of the fortnightly tidal scale (spring and neap tides) and local processes (upwelling and tidal-topographic mixing) that shape planktonic assemblages in the Strait. To do so, an oceanographic cruise was taken in early autumn 2008 with a high-resolution grid sampling and spring/neap tidal conditions. The planktonic features were captured using different automatic and semi-automatic techniques of plankton analyses (flow cytometry, FlowCAM, LOPC and Ecotaxa) that allowed covering a wide range of sizes of the community from pico- to mesoplankton. The SG was sectorized into two clusters based on the biogeochemical and main water column properties. Cluster 1 (CL1) covered shallow productive areas around Cape Trafalgar (CT). CL1 presented higher concentrations of chlorophyll and nutrients, and phytoplankton was mostly represented by *Synechococcus* and coastal diatoms while zooplankton had the highest percentage of meroplankton (31%). In contrast, cluster 2 (CL2) covered open ocean waters and presented more oligotrophic features, i.e. nitrogen-depleted waters with lower chlorophyll concentrations and a picoplankton community dominated by *Prochlorococcus* and holoplankton predominance in mesozooplankton. Under early autumn conditions with overall nutrient-depleted and stratified waters, the CT area emerges as an ecosystem where the constant tidal mixing and nutrients supply is coupled with an active production also being favored by high residence times and finally shaping a plankton community with unique features in the area.

Keywords: plankton community; Strait of Gibraltar; FlowCAM; Ecotaxa; image analysis; size spectra.

Introduction

The SG is the only connection between the Mediterranean Sea and the Atlantic Ocean, therefore, it is a crucially important place for assessing potential drivers of the biogeochemical and hydrological budgets of the Mediterranean basin and their effect on the global circulation (Candela, 2001; Izquierdo & Mikolajewicz, 2019). The SG is characterized as a narrow passage that is only 14km wide and 280m in depth in its shallowest area, the Camarinal Sill. The circulation through the SG can be represented as a two-layer inverse-estuarine exchange with surface inflowing Atlantic waters and deep outflowing Mediterranean waters (Armi & Farmer, 1985). This overall pattern presents a high hydrodynamic variability that is effectuated by the tides, including a complex array of energetic undulatory phenomena due to the interaction between tidally-forced flows and the sharp topography of the Strait (Bruno *et al.*, 2002; García Lafuente *et al.*, 2002; Macías *et al.*, 2006). These intense hydrodynamics with a prominent role of the large amplitude internal waves has been described as the main driver for biogeochemical patterns in the SG and Alboran Sea (Vázquez-Escobar *et al.*, 2009; Ramírez-Romero *et al.*, 2014). Tidal mixing and arrested internal waves above the Camarinall Sill modify the inflowing oligotrophic Atlantic waters, leading coastal patches advection towards the channel and later towards the Alboran Sea (Macías *et al.*, 2007a; Ramírez-Romero *et al.*, 2014; Gómez-Jakobsen *et al.*, 2019).

The oligotrophic inflow of Atlantic waters from the Gulf of Cadiz is mainly composed of oceanic picophytoplankton such as *Prochlorococcus* and *Synechococcus* (García *et al.*, 1994; Echevarría *et al.*, 2009; León *et al.*, 2015; Amorim *et al.*, 2016; González-García *et al.*, 2018). On the other hand, the more productive waters of the northern Atlantic shore and the Alboran Sea are dominated by microplankton that is composed of primarily diatoms (Gómez *et al.*, 2000; Gomez *et al.*, 2004; Reul *et al.*, 2005; García-Gómez *et al.*, 2020). The confluence of these water masses in the SG results in a marked horizontal gradient in terms of primary production and associated planktonic assemblages.

Higher trophic levels of the community (mesozooplankton) are also affected in the region by physical forcing and mesoscale processes (Macías *et al.*, 2010; Van Haren, 2014; Yebra *et al.*, 2017, 2018). Besides diel vertical migration (Frassetto *et al.*, 1962), frontal areas accumulate biomass and alter the composition of the community forced by internal wave events (Macías *et al.*, 2010; Garwood *et al.*, 2020). Overall, the main channel is primarily dominated by medium sized copepods (Vives *et al.*, 1975; Macías *et al.*, 2010). Nevertheless, under warmer conditions, there is an increase in the abundances of cladocerans in both sides of the SG (Sampaio De Souza *et al.*, 2011; Llope *et al.*, 2020) with *Penilia avirostris* being the most frequent species.

Although planktonic assemblages in the SG and adjacent areas have been fairly studied, there is a lack of a general high resolution description at synoptic scales. In addition, there are only a small number of detailed taxonomic descriptions and none cover the entire plankton size spectra. The taxonomic analyses are often hindered because they require a high taxonomic qualification and are particularly very time consuming. Recently, however, the use of automatic and semiautomatic plankton analysis techniques have become more popular because they enable improving the efficiency of these taxonomic analyses (Hu & Davis, 2006; Culverhouse *et al.*, 2006; Zheng *et al.*, 2017).

The primary objective of this work was to reduce insufficiencies in the knowledge about the drivers and spatial patterns of a planktonic community in a highly dynamic system such as the Strait of Gibraltar. The authors analysed the role of fortnightly tidal scales (spring/neap tides) versus local processes (such as wind-driven upwelling or tidal-topographic mixing) shaping the planktonic assemblages in the Strait. This work aims to assess, for the first time, the variability in the structure of the planktonic assemblages with a detailed spatial resolution, covering from nanoplankton to mesozooplankton with a combination of automatic and semiautomatic methods. The specific objectives include: a) assessing the fortnightly variability of planktonic assemblages in the SG, b) describing the spatial patterns of the communities through a regionalization of the study area, and c) detailing the composition of the planktonic community with a combination of different automatic methodologies.

Materials and Methods

Field Sampling

Data were aggregated during a cruise between 16 September and 9 October 2008 aboard the research vessel B/O Sarmiento de Gamboa. The study area covered the Strait of Gibraltar and the western Alboran Sea with a total of 75 sampling stations. These stations were sampled twice under two different tidal conditions: spring and neap tides (Fig. 1).

The CTD profiles were taken in each sampling station. Temperature, conductivity, oxygen, turbidity, and fluorescence were recorded from surface to bottom. The Atlantic Mediterranean Interface (AMI) was identified by the 37.3 isohaline as defined by Sala (2021). The stability of the water column was assessed by examining Brunt-Väisälä frequency (N^2) (Sabetta *et al.*, 2008; Roselli & Basset, 2015) and defining the mixed layer depth (MLD) where N^2 is maxima. N^2 was calculated using "oce" package for R (R Core Team, 2008; Kelley & Richards, 2016)

Seawater from fixed discrete depths (5, 25, 50, 75, 150, 200 m) and deep chlorophyll maxima (DCM) was collected using Niskin bottles on a rosette sampler. Total chlorophyll (TChla) was estimated from 1 L samples filtered through Whatman GF/F filters (0.7 µm). Fractionated chlorophyll (FChla) was sampled by filtering 5 L of seawater through a 20 µm nylon mesh and collecting the fraction retained with filtered seawater. This fraction was filtered again (Whatman GF/F). The total and fractionated chlorophyll filters were kept in the dark and frozen on board at -20 ºC until the analysis in the laboratory. The chlorophyll content in the TChla and FChla samples was determined by fluorometry following the protocol by Yentsch & Menzel (1963) and modified by Holm-Hansen & Hewes (2004). The percentage of active chlorophyll (AChla) was estimated on board following the procedure described in Macías *et al.* (2008b) using a pulse amplitude modulated (PAM) fluorometer (PhytoPAM©) that estimates the proportion of total chlorophyll within active PS II (Kolbowski & Schreiber, 1995).

Inorganic nutrients samples were filtered (Whatman GF/F) and stored at -20 ºC for their analysis in the laboratory. The concentrations of nitrate, silicate, and phosphate were measured using a Skalar San ++ System autoanalyser following Grasshoff *et al.* (1983).

Particles for microplankton analysis were concentrated on board from 5 L of seawater by filtration using a 10 µm mesh. Mesoplankton samples were collected with a 250 µm mesh Bongo net. Double oblique hauls were carried out from the surface to 200 m (or bottom depth in shallower stations). All samples were fixed (formaldehyde f. c. 4%) and stored in darkness for analysis. Samples for pico-, nano-, and microplankton were taken at 25 m and analysed on board.

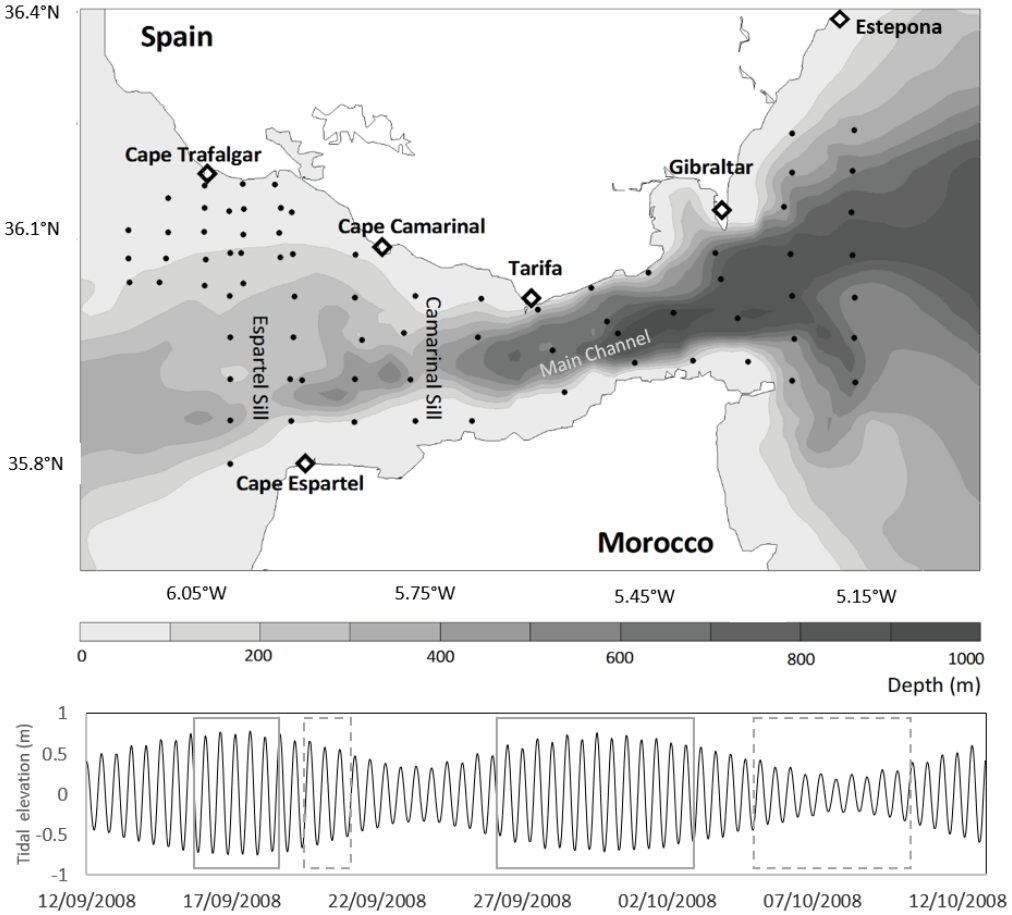

Fig. 1: Top: Map of the study area, sampling stations are denoted by black dots, grey scale represents depth (m). Bottom: Tidal elevation (m) during the cruise. Solid and dashed boxes mark samplings made during spring and neap tides respectively.

Plankton samples processing

Pico and nanoplankton analysis

Samples for a pico and nanoplankton analysis (20 ml) were fixed with 5 ml of fixation cocktail (5% formaldehyde, 0.25% glutaraldehyde). A nano and picoplankton analysis was conducted on board with a FACSaria (BD) flow cytometer using MiliQ water as the evolving flow. Each sample was pumped at 80 µl min-1 during seven minutes and analysed twice with different settings that were intended to properly characterize the pico and nanoplankton.

For the nanoplankton species, the SSC signal was converted to biovolume (BV, in μm^3) using the empirical relationship BV = 0.0525 * SSC - 24.688 ($r^2 = 0.89$, n = 3). The regression equation was obtained by measuring the BV of different cultures of phytoplankton by optic imagery and comparing the results to the SSC signal.

Microplankton analysis

The abundance, biovolume, and taxonomic composition were analysed using a Flow Cytometer and Microscope (FlowCAM®, Fluid Imaging Technologies, Yarmouth, ME, USA) (Sieracki *et al.*, 1998). Concentrated samples were divided into two fractions with a 100 µm mesh. Both of them were analysed in auto image mode (20 photographs per second, flow rate over 1 ml min^{-1}). The fraction with particles larger than 100 µm was prefiltered with a 250 µm mesh to avoid obstructions and used for analysis at x40. The remaining fraction (10 – 100 µm) was analysed at x100 magnification. All samples were pumped through the FlowCAM for at least 30 minutes. When the counted particles were less than 400 (<10% counting error, Lund *et al.* (1958)), the entire sample was analysed.

Images were examined by *VisualSpreadSheet* 2.4.6. Invalid vignettes (bubbles, detritus, and duplicated images) were first removed from the database through visual recognition. Plankton images were classified into groups according to their taxonomic class, size, and shape as in Morillo-García *et al.* (2014). The sorting was performed with *VisualSpreadSheet* automatic classification based on images libraries. Each group was analysed after automatic classification and corrected by visual inspection, placing wrong vignettes manually into their proper groups.

VisualSpreadSheet provided an estimation of cell volume based on the Equivalent Spherical Diameter (ESD). Considering all the cells spherical can bias the biomass estimation when particles are cylindrical (most of diatoms) or photographed in different orientations (Álvarez *et al.*, 2012) which would lead to an overestimation of

volume. The authors used the aspect ratio for each cell (major to minor axis ratio also given by the software) to correct the spherical volume into ellipsoidal volume according to Herman (2009).

Additionally, some samples were selected and inspected under the inverted microscope in order to identify the species' composition of the major groups used to classify the FlowCAM images.

Mesoplankton analysis

Mesoplankton samples were analysed with a submersible Laser Optical Plankton Counter (LOPC) (Herman *et al.*, 2004) adapted for laboratory work which recorded all of the planktonic organisms present in the samples from 250µm to 3000µm. Before the analysis, the pumping system was inspected for the presence of bubbles. Each sample was first observed in order to remove organisms larger than 3 mm to avoid occlusions. Data for SEP (Single Element Particle) and MEP (Multi Element Particle) were processed with R software (R Core Team, 2008) following directions in Herman (2009). As FlowCAM, LOPC also measures the cross- sectional area for each particle, data were corrected as described above. Fixed samples were not suitable for distinguishing marine snow from LOPC (Checkley *et al.*, 2008; Jackson & Checkley, 2011), therefore, in order to obtain taxonomic information, fourteen samples were imaged with a scanner (*Epson Perfection 4490 Photo*) at 3200 dpi and processed with *Zooprocess* (Gorsky *et al.*, 2010). Automatic prediction and manual validation of all of the vignettes were made with Ecotaxa (Picheral *et al.*, 2017). Mesozooplankton (heterotrophic plankton > 200 µm) was classified into major groups. Copepods were grouped into four orders (Razouls *et al.*, 2005) and classified in three different size ranges: small copepods (< 1 mm), medium copepods (1mm – 2mm), and large copepods (>2mm) (Bacha & Amara, 2009; Frangoulis *et al.*, 2017).

Data processing

The particles' biovolume was converted to biomass with the equations proposed by Verity *et al.* (1992) for nanoplankton, Montagnes *et al.* (1994) for microplankton, and Alcaraz *et al.* (2003) for mesoplankton. They were subsequently grouped into octaves size intervals (Ln2) and normalized according to Platt and Denman (1978) and Blanco et al. (1994):

$$NB = (N \times S)/(Smax - Smin) \qquad \textbf{Equation 1}$$

where NB is the normalized biomass in pg C m^{-3} mm^{-3}, and N is the total abundance in the size interval (Smin to Smax) with S as its mean individual biomass.

Plankton NBSS (Normalized Biomass Size Spectrum) was presented by the log-linear model (Platt & Denman, 1978) and constructed by using the least-square regression according to the following equation (Kerr & Dickie 2001):

$$log(NB) = \alpha \pm \beta log(S) \qquad \textbf{Equation 2}$$

with log to the base 10, where α is the intercept and β is the slope of regression. The NBSS parameters such as the intercept and slope values can be used to summarise plankton community properties. A higher intercept value means a greater abundance of organisms and system productivity and vice versa (Kerr & Dickie 2001, Jennings & Brander 2010). The slope is determined by the energy transfer efficiency and number of trophic levels (Zhou, 2006). A slope value of -1 represents the hypothetically steady-state community or system when size is expressed in terms of volume which means biomass is evenly distributed in different size fractions (Sheldon *et al.*, 1972). A slope value flatter than -1 means more biomass occurs at larger size fractions and vice versa according to Macpherson & Gordoa (1996).

Statistical analysis

Stations were classified on the basis of their hydrographic and biogeochemical conditions by a k-means clustering algorithm. Variables measured at discrete depths (temperature, salinity, TChla, % FChla, nitrate, nitrite, ammonium, and silicate) were averaged down to the MLD for the analysis. The number of clusters was validated using the NbClust R Package (Charrad *et al.*, 2014) which evaluates the appropriate number of clusters among several indexes. The majority rule was used to choose that our K would be two (validated by 12 indexes).

The non-parametric Kruskal-Wallis test was run to assess differences between clusters and environmental factors. Statistical analyses was performed using IBM SPSS Statistics 22 software.

Results

Physicochemical variables

Biogeochemical variables followed a common pattern showing maxima in coastal stations also being significantly higher during spring tides (Fig. 2, Table S1). TChla ranged from 0.1 to 4.5 mg m^{-3} with an average concentration of 1.3 mg m^{-3} (± 1.2 Standard Deviation, SD) during spring tides and 0.7 (± 0.4 SD) during neap tides. FChla scored 87% of TChla in spring tides at coastal stations while concentrations during neap tides and oceanic stations were lower (Table S1). Nitrate and nitrite concentrations presented a similar distribution with concentrations ranging from 0 to 25 µM for nitrate and 0.1 to 0.9 µM for nitrite (Fig. 2).

Based on the physical and biogeochemical conditions in the water column, two regions were detected (Fig. 3). CL 1 stations markedly presented the highest concentrations of TChla and the percentage of FChla, nitrate, nitrite, and ammonium compared to CL2 (Fig. S1, Table S1). Furthermore, mean AChla in CL1 was 73%, signifi-

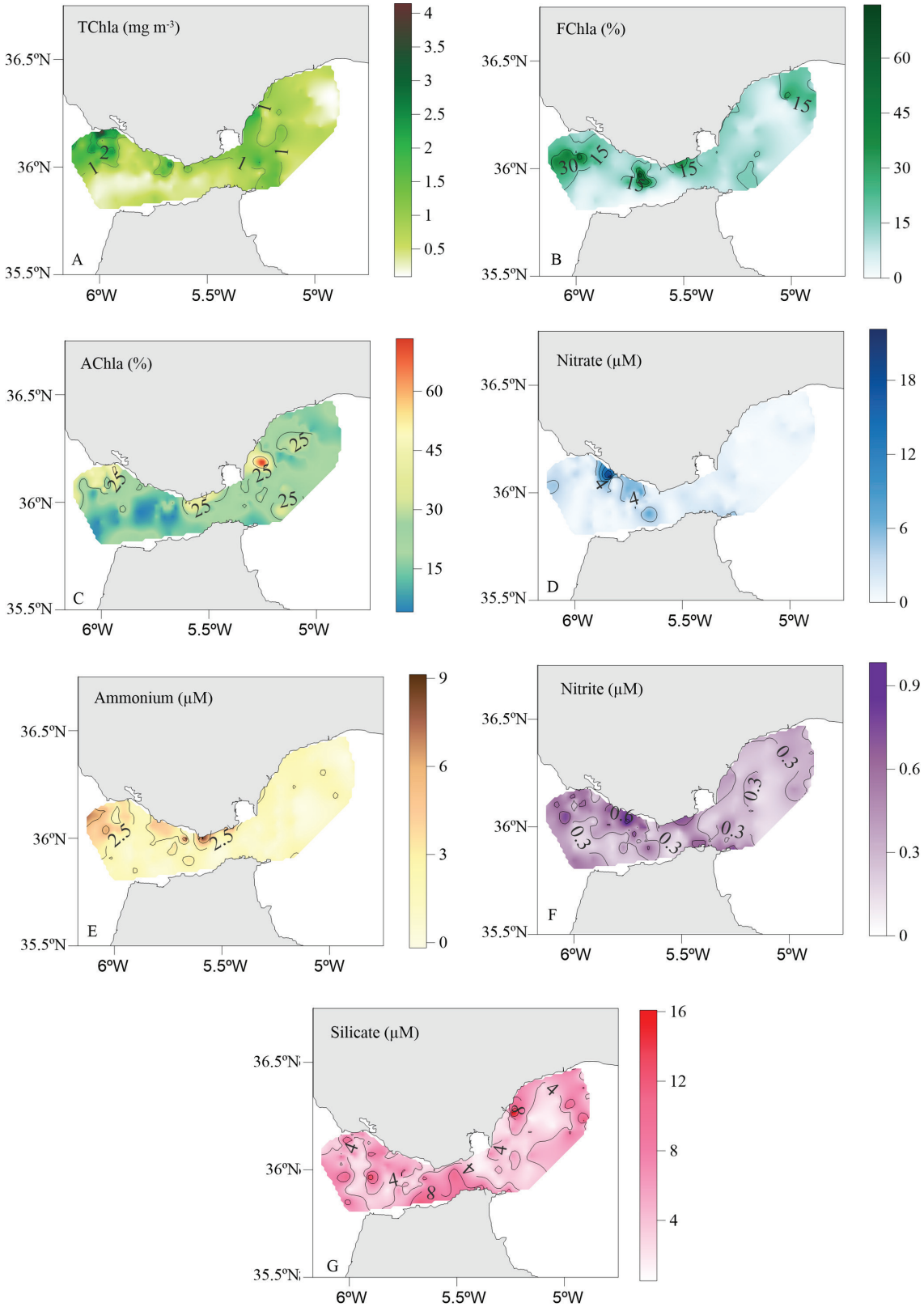

Fig. 2: Biogeochemical variables averaged within the MLD in the SG during the cruise. A) TChla (mg m^{-3}), B) FChla (% of TChla) C) AChla (% of TChla) D) Nitrate (µM) E) Ammonium (µM) E) Silicate (µM) F) Nitrite (µM) G) Silicate (µM).

cantly higher ($p < 0.005$) than CL2 (53%), although this variable was not included in the cluster analysis due to the lack of data in some stations. All of the variables that were analysed except silicate were significantly different between clusters ($p < 0.005$) according to the Kruskal-Wallis test.

Most of CL1 stations were located in coastal areas at the Atlantic sector mainly from Cape Trafalgar (CT) to Tarifa. However, some of them were placed in the middle of the main channel (Fig. 3). CL2 primarily covers the main channel and the NW Alboran Sea. This pattern of distribution is very similar between spring and neap tides with the exception that some stations at the east side classed as CL1 during spring tides and CL2 during neap tides.

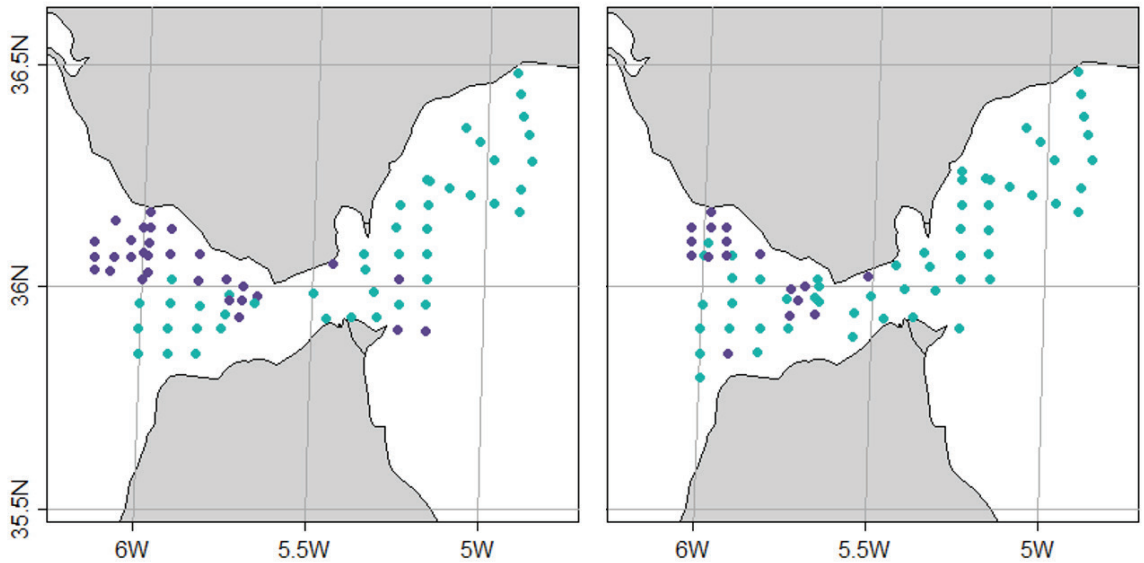

Fig. 3: Distribution of the sampling stations classed in two clusters by k-means method. Left map shows stations sampled in spring tides and right neap tides. Cluster 1 and 2 signed by purple and blue dots respectively.

Plankton size structure

The spatial distribution of particles presented maximum concentrations and mass in the area close to the CT and coastal stations (CL1). Also, abundances were significantly higher during spring tides ($p < 0.01$) (Table S2, Table S3, Table S4).

The total planktonic biomass was dominated, on average, by the mesoplanktonic fraction with an average 61% of the community total biomass (Table 1). This effect is more marked for samples in CL1 (Table S4, Fig. 4). The variability observed in the percentage of tripton in the samples was noteworthy. The microplanktonic fraction had an average of 30% non-living particles, 42% (±20.94 SD) in CL1 and 26% (±23.19 SD) in CL2. On the other hand, the mesoplanktonic fraction presented ca. 47% of tripton (±13.5 SD) in total, 44% (±7.8 SD) in CL1 and 47% (±17.1 SD) in CL2. The total seston weight was significantly higher for micro and mesoplanktonic fraction ($p < 0.001$) during spring tides, however, no differences were ascertained between plankton biomass in any fraction.

The spatial distribution of NBSS slopes showed, in general, more negative slopes from west to east and from the south to the north of the Strait. Coastal stations from the CT area to Tarifa had more presence of large cells than the rest of the stations (-1.34 and -1.27 mean global slopes of the NBSS, respectively). However, there were no significant differences determined among slopes during the spring or neap tides nor between clusters (Table 2).

Community composition

Pico and nanoplankton

Picoplankton densities were not clearly different among tidal phases (Fig. S2). During spring tides, the authors recorded total picoplankton cell densities reaching 84000 cells mL^{-1}. *Prochlorococcus* was the dominant group in picoplankton with a mean abundance higher than *Synechococcus* (27066 and 18258 cells mL^{-1}, respectively) while *Cryptophytes* are less abundant (164 cells mL^{-1}). During neap tides, there was an opposite pattern with *Synechococcus* doubling *Prochlorococcus* abundance (5928 and 2110 cells mL^{-1}, respectively). It is also remarkable that picoplankton cell densities were lower ($p < 0.001$) during neap tides than spring tides.

Synechococcus and *Prochlorococcus* biomass (Fig. S2) displayed a patchy distribution in spring tides and

Table 1. Plankton biomass (mgC m^{-3}) during spring and neap tides and between clusters. Mean ± standard deviation.

		Nanoplankton (Mean ± SD)	Microplankton (Mean ± SD)	Mesoplankton (Mean ± SD)
Spring	CL1	30.5 ± 8.20	23.03 ± 8.34	103.62 ± 18.81
	CL2	28.9 ± 10.42	32.26 ± 51.52	33.19 ± 10.27
Neap	CL1	17.63 ± 0	59.57 ± 51.96	221.8 ± 0
	CL2	21.3 ± 8.76	31.02 ± 40.41	110.30 ± 87.28
Total	CL1	30.5 ± 8.20	41.30 ± 36.99	165.61 ± 124.92
	CL2	24.4 ± 9.93	31.64 ± 45.07	64.03 ± 61.16

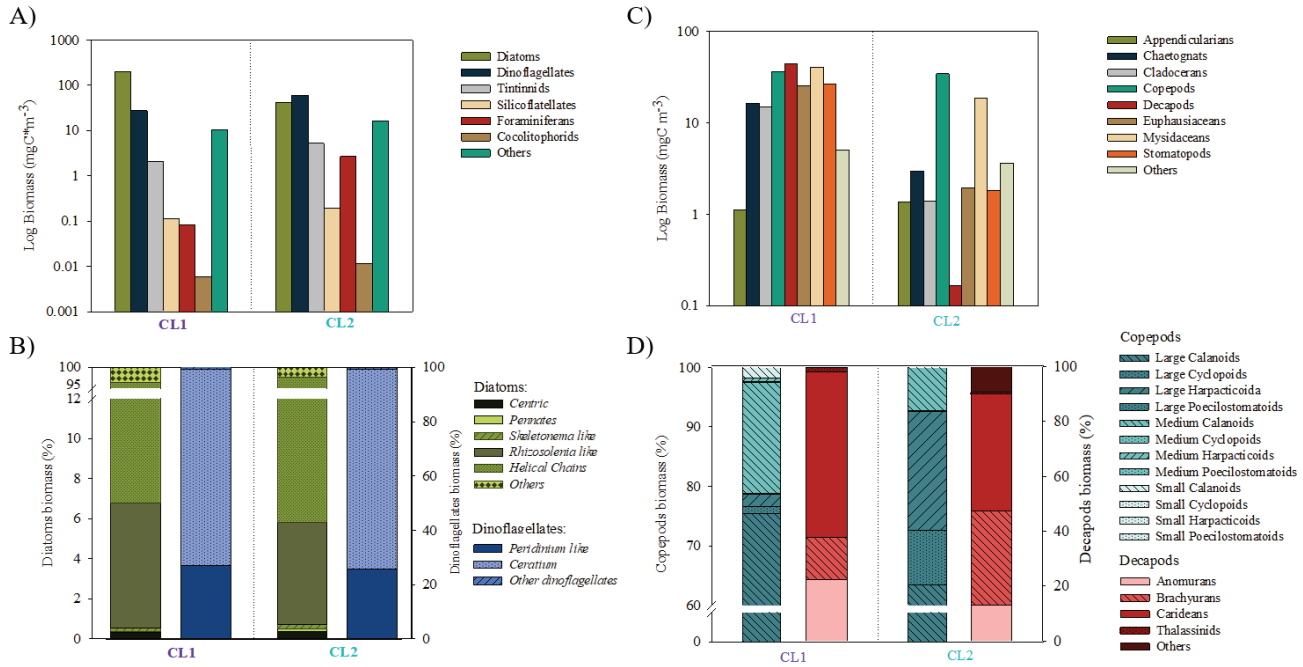

Fig. 4: Mean plankton biomass by groups in the clusters. A) Biomass of the microplankton major groups (mgC m^{-3}) in the clusters. B) Diatoms (left axis) and dinoflagellates (right axis) composition (% biomass) between clusters. C) Mesoplankton major groups biomass (mgC m^{-3}) distribution into the clusters. D) Copepods (left axis) and decapods (right axis) composition (% biomass) between clusters.

was more homogeneous in general during neap tides. However, through neap tides, the *Cryptophytes* had a distribution in bands across the Strait reaching higher values in the channel than those recorded during spring tides.

Picoplankton showed maximum abundance and biomass on the west side of the SG. *Prochlorococcus* biomass increased from north to south whereas *Synechococcus* presented maximum scores (abundance and biomass) in the north west coast during spring tides and the north east coast (close to Estepona) during neap tides.

Picoplankton presented significant differences ($p<0.001$) between clusters (Table 2, Table S5). *Synechococcus* was dominant in terms of biomass in CL1 over CL2 (59 and 38 mgC m^{-3}) while *Prochlorococcus* had double biomass in CL2 over CL1 (53 and 24 mgC m^{-3}). *Cryptophytes* were also different between clusters ($p<0.001$) attending to their abundance; they were two times higher in CL1 over CL2 (72 and 38 cells mL^{-1}).

Microplankton

Microplankton abundances demonstrated differences between spring and neap tides (Fig. S3) ranging from 12.3 cell mL^{-1} as the maximum density in neap tides to 52.4 cell mL^{-1} in spring tides. In addition, all of the major microplankton groups had higher abundance (also biomass) during spring tides than neap tides (Table S3). The most important group in all stations, both in spring and neap tides, was diatoms that represented an average of 79% from the total phytoplankton (± 12% SD) followed by dinoflagellates. The increment in foraminiferans during neap tides is outstanding. Within diatoms, those species forming helical chains (e.g., *Guinardia striata, Chaetoceros debilis*) were the group with higher densities (4.7 cell or chains per mL in spring tides) and biomass followed by large individual single cells or linear chains (e.g., *Rhizosolenia* and *Proboscia* type, *Leptocylindrus* and *Lauderia* chains) (Table S3). The abundance of diatoms during spring tides was twice that of neap tides. Additionally, this difference was even higher attending to biomass values (Table S3).

Although all of the groups showed maximum abundances in the stations located in the CT area, the spatial distribution of microplankton biomass and the composition of the communities between clusters were similar (Fig. 4). The most remarkable differences concern CL2 which is the cluster with the higher biomass of foraminiferans. Within major phytoplankton groups, there are no variances in the dominant group ("Helical chains" and *Ceratium* in diatoms and dinoflagellates respectively). However, CL1 showed a higher biomass of "Lineal chains" and *Rhizosolenia* like diatoms while CL2 had lower biomass of that group but an increment of "Helical chains", *Skeletonema* like, and pennates (Fig. 4).

Mesoplankton

Copepods were the primary group in terms of abundance (Fig. 4) during both spring and neap tides (Table S4) and dominated CL1 and CL2. However, in terms of biomass, there were some differences among clusters. CL1 presented higher meroplankton biomass (31% of meroplankton vs. 4% in CL2). Consequently, decapods and mysidaceans were dominant in CL1 while copepods

Table 2. H statistic, degrees of freedom and the P value resulting of Kruskal-Wallis test between clusters and tidal phase. ** p < 0.05, ***p < 0.01.

	Cluster			Tidal phase		
	H	df	P value	H	df	P value
Size spectra						
General slope (2 – 3000 µm)	2.81	1	0.09	0.67	1	0.41
Nanoplankton slope (2 – 20 µm)	2.35	1	0.12	1.08	1	0.29
Microplankton slope (20 - 200 µm)	2.92	1	0.09	0.39	1	0.53
Mesoplankton slope (200 – 3000 µm)	3.07	1	0.08	1.72	1	0.19
Particles biomass (mg m^{-3})						
Nanoplankton (2um – 20µm)	1.24	1	0.27	7.49	1	***
Microplankton (20 - 200 µm)	10.04	1	***	0.00	1	0.98
Mesoplankton (200 – 3000 µm)	24.92	1	***	0.68	1	0.41
Plankton groups biomass (mg m^{-3})						
Synechococcus	12.01	1	***	50.05	1	***
Prochlorococcus	22.70	1	***	78.65	1	***
Cryptophytes	0.17	1	0.68	2.77	1	0.10
Single rounded cells	2.94	1	0.09	1.06	1	0.30
Pennates diatoms	1.00	1	0.32	0.14	1	0.70
Skeletonema like	4.64	1	**	0.56	1	0.45
Lineal diatom chains and *Rhizosolenia* like	3.03	1	0.08	9.47	1	***
Helical diatom chains	2.56	1	0.11	0.54	1	0.46
Other diatoms	4.64	1	**	1.71	1	0.19
Peridiniales	3.88	1	**	1.59	1	0.21
Ceratium/Neoceratium	2.56	1	0.11	3.14	1	0.08
Other dinoflagellates	0.50	1	0.48	0.00	1	1.00
Tintinnids	0.20	1	0.65	0.04	1	0.84
Silicoflagellates	1.55	1	0.21	1.11	1	0.29
Foraminiferans	1.19	1	0.28	0.50	1	0.48
Coccolitophores	0.00	1	1.00	0.00	1	1.00
Amphipods	1.50	1	0.22	1.50	1	0.22
Appendicularians	0.53	1	0.46	5.60	1	***
Ascidians	0.12	1	0.72	1.00	1	0.31
Bryozoans	1.32	1	0.25	0.32	1	0.56
Chaetognaths	0.06	1	0.80	0.25	1	0.61
Cirripeds	4.81	1	**	0.05	1	0.81
Cladocerans	2.16	1	0.14	0.25	1	0.61
Large Copepods	0.09	1	0.75	4.11	1	0.04
Medium Copepods	0.04	1	0.82	0.11	1	0.73
Small copepods	0.00	1	1.00	0.45	1	0.49
Decapods	1.50	1	0.22	0.10	1	0.75
Doliolids	1.00	1	0.31	0.04	1	0.83
Scaphopods	1.00	1	0.31	2.40	1	0.12
Euphausiaceans	0.88	1	0.34	0.02	1	0.86
Hydromedusa	1.00	1	0.31	0.00	1	1.00
Limacinids	0.09	1	0.75	1.00	1	0.31
Molluscs	0.20	1	0.65	0.15	1	0.69
Nauplii	0.12	1	0.72	0.11	1	0.73
Ophiuroideans	1.92	1	0.16	0.77	1	0.38
Ostracods	0.02	1	0.88	0.00	1	1.00
Polychaets	0.12	1	0.72	2.45	1	0.11
Salps	0.01	1	0.91	1.00	1	0.31
Siphonophores	1.32	1	0.25	1.02	1	0.31
Unidentified	0.02	1	0.88	1.38	1	0.23

still dominated CL2 (52% vs. 22% in CL1).

All of the main groups demonstrated higher biomass in CL1 than CL2. The Copepods group was the only group without differences in terms of total biomass. Calanoid copepods were dominant in terms of abundance (Table S6). In particular, large calanoids were the principal group within the copepods (> 63%) followed by medium calanoids and small calanoids in CL1, however, in CL2, large harpacticoids were the second predominant group (Fig. 4). The decapod biomass was mainly attributed to carideans (60 – 40 % for CL1 and CL2, respectively) followed by anomurans in CL1 and brachyurans in CL2.

Discussion

The Strait of Gibraltar and surrounding areas is a complex region with contrasting productivity sectors (Navarro & Ruiz, 2006; Macías *et al.*, 2007b; Mercado *et al.*, 2016; Yebra *et al.*, 2017, 2018; Sala *et al.*, 2018; Gómez-Jakobsen *et al.*, 2019). In the present study, it was divided into two regions according to the hydrographical and biogeochemical properties of the water column with a derived contrasting response and features of the planktonic communities.

This work was performed under very oligotrophic conditions and stratification of the water column (Fig. 3, Fig. S1, Fig.S4). Therefore, it is assumed that the proposed regionalisation could be representative and relevant during the stratified season extending from July to October in this area according to satellite work (Mercado *et al.*, 2016; Sala *et al.*, 2018) and former studies (Prieto *et al.*, 2009).

Spatial variability

The region defined by CL1 is mainly characterized by high concentrations of chlorophyll (and % in large cells) and the higher levels of nitrate, nitrite, and ammonium. The stations that were divided and categorized as CL1 are located mainly at the eastern north coast of the SG including Cape Trafalgar. This is a productive zone due to an upwelling process and constant nutrient supply due to tidal mixing (Vargas-Yáñez *et al.*, 2002) and also favoured by high residence times of the water masses ca. three days (Vázquez-Escobar *et al.*, 2009; Bolado-Penagos *et al.*, 2020).

Planktonic communities within this area are typical of productive waters with flatter slopes of the biomass size spectrum meaning a larger contribution to biomass by large organisms than in the other stations. This issue is corroborated by the percentage of chlorophyll contained in larger cells and also by the large proportion of meroplanktonic larvae in the CL1 mesozooplankton biomass (Fig. 4). Furthermore, the biomass of the three planktonic fractions analysed is the highest of the study area. The picoplankton presented the highest levels in CL1 and was mainly represented by *Synechococcus* in the area which is in agreement with previous studies (Reul *et al.*, 2005; Echevarría *et al.*, 2009; González-García *et al.*, 2018). However, the nanoplanktonic fraction did not show any spatial pattern in the area which accorded with previous observations (Rodríguez *et al.*, 1998). Previous work stated that the smaller fractions dominate the biomass of planktonic communities here (Reul *et al.*, 2002; Echevarría *et al.*, 2009). However, our results show that the mesoplanktonic fraction represented the largest contribution to the planktonic biomass (Table 1).

Diatoms were the primary group in the phytoplankton biomass in CL1. The leading group was Helical chains involving species that are characteristic from neritic areas such as *Guinardia striata* and *Chaetoceros debilis* (Cupp, 1943; WoRMS Editorial Board, 2021) and aligning with previous results obtained in the same area (Gómez *et al.*, 2000; Echevarría *et al.*, 2002). The second group in biomass for CL1 was Lineal chains and *Rhizosolenia* like what is constituted by species with large individuals and linear chains of large cells like *Rhizosolenia setigera* that preferentially inhabits coastal waters (Cupp, 1943; EOL, 2011). The percentage of meroplanktonic larvae (31% in the biomass) in the mesozooplankton community also reveals the productive and coastal imprint of CL1.

CL2 represents stations where nutrients are depleted and the production is low. At the Mediterranean side of the Strait, it was unexpectedly found mostly stations classed as CL2. Although this is an area with a quasi-permanent coastal upwelling, persistent easterly winds can prevent this process (Reul *et al.*, 2005; Macías *et al.*, 2007b, 2008a; Echevarría *et al.*, 2009). Therefore, under these conditions, the easternmost area was more influenced by the inflow of oligotrophic Atlantic waters by the SG through the Atlantic Jet. Appendicularians were the only group in the zooplankton with a higher biomass in CL2 than in CL1 which is in accordance with previous observations in the area (Vives *et al.*, 1975). However, the authors' expected to find a prevalence of Appendicularians in CL1 over CL2 due to their trophic regime, Vives *et al.* (1975) attributed their presence in this area to the regime of winds and currents in the region.

Additionally, some stations classed as CL1 were found located on the western side only during spring tides. These stations could be the result of the suction of enriched coastal waters produced during spring tides (Macías *et al.*, 2008b; Ramírez-Romero *et al.*, 2014).

Fortnightly variability

This work illustrates the variability of planktonic communities in the Strait of Gibraltar under a spatial perspective but also differences between spring or neap tides in a fortnightly scale. The results corroborate previous studies signing the enhancement of productivity during spring tides due to the mixing processes related with internal waves (Macías *et al.*, 2006; Bartual *et al.*, 2011). In this situation, there is a predominance of *Prochlorococcus* in picoplankton communities and the highest abundances of micro phytoplankton over the entire Strait of Gibraltar. During spring tides, there is also an increase in

the biomass of all microplanktonic groups. The input of nutrients due to the mixing could possibly be related to the increment in the productivity of the smaller planktonic groups matching the description made by Margaleff in the pattern of phytoplankton succession (Margalef, 1978). This is in accordance with the results of previous studies in the area (Macías *et al.*, 2013). The results also suggest that, in the case of dinoflagellates, the cell densities are similar but not the biomass so spring tides could favour species with larger cell size (Table S3). Further research is required for establishing if there is a difference in body size for the same species or if there is a shift in the species composition between spring and neap tides.

Previous authors stated that physical forcing was the main driver of the distribution of the biomass and some taxonomic groups of zooplankton in the Strait (Macías *et al.*, 2010). However, the results show only chaetognaths were more abundant during spring tides regarding fortnightly variability. Nonetheless, the highly variable and intense hydrodynamics over all of the SG drives the short residence time of the waters and does not allow observing the succession after intense mixing of biological communities. There is an exception in some locations such as the CT area that is characterized by a residence time of several days (Bolado-Penagos *et al.*, 2020)) and coastal communities properly coupled with the supply of nutrients.

In addition to the fortnightly processes over planktonic assemblages, there is also an influence of atmospheric forcing over the community via wind-driven upwelling process. The northern coast of the Alboran Sea used to present an outstanding primary production in the Mediterranean due to quasi-permanent upwelling (Prieto *et al.*, 1999; Sarhan & Vargas-Yáñez, 2000; Mercado *et al.*, 2005; Macías *et al.*, 2007b; Echevarría *et al.*, 2009). However, the cruise occurred during a weakening event of the upwelling (Mercado *et al.*, 2012; Ramírez-Romero *et al.*, 2014), and the signs of productivity expected in the area were not observed.

This study presents, for the first time, a detailed spatial resolution description of the plankton community in the SG from nanoplankton to mesoplankton and also including tidal variability. This work enhances the perception on the western north coastal region as an "oasis" area where the constant supply of nutrients is coupled with an active production also being favoured by the high residence time of the waters. Through a taxonomic analysis and the NBSS, the authors also showed the importance of mesozooplankton biomass on the global plankton community and particularly of meroplankton in shallow areas around Cape Trafalgar. These areas emerge as a crucial ecosystem especially during the less productive seasons such as late summer/fall. These processes configure the coastal planktonic assemblages in the CT area with unique features in the Southern Spain Mediterranean shores.

Acknowledgements

This work is dedicated to the memory of our beloved colleague, Luis M. Lubián, who was in charge of the flow cytometry analysis during the cruise. We thank the UTM (Unidad de Tecnología Marina, CSIC) and the crew of R/V Sarmiento de Gamboa during Gibraltar 08. We would like to extend our deepest gratitude to all of the colleagues who collaborated during the cruise. We thank L. Yebra for her comments on an earlier version of the manuscript. This project was funded by the Spanish Ministry of Science and Innovation (CTM2008-06124) and has been also supported by the Andalusian Research Group "EDEA" PAI RNM-214. NVP was supported by a PhD scholarship from the same institution (BES-2009-013347).

References

Alcaraz, M., Saiz, E., Calbet, A., Trepat, I., Broglio, E., 2003. Estimating zooplankton biomass through image analysis. *Marine Biology*, 143 (2), 307-315.

Álvarez, E., López-Urrutia, Á., Nogueira, E., 2012. Improvement of plankton biovolume estimates derived from image-based automatic sampling devices: application to FlowCAM. *Journal of Plankton Research*, 34 (6), 454-469.

Amorim, A.L., León, P., Mercado, J.M., Cortés, D., Gómez, F. *et al.*, 2016. Controls of picophytoplankton abundance and composition in a highly dynamic marine system, the Northern Alboran Sea (Western Mediterranean). *Journal of Sea Research*, 112, 13-22.

Armi, L., Farmer, D., 1985. The internal hydraulics of the Strait of Gibraltar and associated sills and narrows. *Oceanologica Acta*, 8 (1), 37-46.

Bacha, M., Amara, R., 2009. Spatial, temporal and ontogenetic variation in diet of anchovy (Engraulis encrasicolus) on the Algerian coast (SW Mediterranean). *Estuarine, Coastal and Shelf Science*, 85 (2), 257-264.

Bartual, A., Macías, D., Gutierrez-Rodriguez, A., García, C.M., Echevarría, F., 2011. Transient pulses of primary production generated by undulatory processes in the western sector of the Strait of Gibraltar. *Journal of Marine Systems*, 87 (1), 25-36.

Blanco, J.M., Echevarría, F., García, C.M., 1994. Dealing with size-spectra: Some conceptual and mathematical problems. *Scientia Marina*, 58 (1-2), 17-29.

Bolado-Penagos, M., González, C.J., Chioua, J., Sala, I., Jesús Gomiz-Pascual, J. *et al.,* 2020. Submesoscale processes in the coastal margins of the Strait of Gibraltar. The Trafalgar - Alboran connection. *Progress in Oceanography*, 181 (October 2019), 102219.

Bruno, M., Juan Alonso, J., Cózar, A., Vidal, J., Ruiz-Caavate, A. *et al.,* 2002. The boiling-water phenomena at Camarinal Sill, the strait of Gibraltar. *Deep-Sea Research Part II: Topical Studies in Oceanography*, 49 (19), 4097-4113.

Candela, J., 2001. Chapter 5.7 Mediterranean water and global circulation. *International Geophysics,* 77, 417-429.

Charrad, M., Ghazzali, N., Boiteau, V., Niknafs, A., 2014. NbClust : An R Package for Determining the. *Journal of Statistical Software*, 61 (6), 1-36.

Checkley, D.M., Davis, R.E., Herman, A.W., Jackson, G.A., Beanlands, B. *et al.,* 2008. Assessing plankton and other particles in situ with the SOLOPC. *Limnology and Ocean-*

ography, 53 (5, part 2), 2123-2136.

Culverhouse, P., Williams, R., Benfield, M.C., Flood, P., Sell, A. *et al.* 2006. Automatic image analysis of plankton: future perspectives. *Marine Ecology Progress Series*, 312, 297-309.

Cupp, E.E., 1943. Marine Plankton Diatoms of the West Coast of North America. University of California Press.

Echevarría, F., García Lafuente, J., Bruno, M., Gorsky, G., Goutx, M. *et al.,* 2002. Physical - biological coupling in the Strait of Gibraltar. *Deep Sea Research II*, 49, 4115-4130.

Echevarría, F., Zabala, L., Corzo, A., Navarro, G., Prieto, L. *et al.,* 2009. Spatial distribution of autotrophic picoplankton in relation to physical forcings: the Gulf of Cadiz, Strait of Gibraltar and Alboran Sea case study. *Journal of Plankton Research*, 31 (11), 1339-1351.

EOL, Encyclopedia of Life, 2011. Rhizosolenia setigera Brightwell 1858. Retrieved December 1, 2021, from http://www.eol.org.

Frangoulis, C., Grigoratou, M., Zoulias, T., Hannides, C.C.S., Pantazi, M. *et al.,* 2017. Expanding zooplankton standing stock estimation from meso- to metazooplankton: A case study in the N. Aegean Sea (Mediterranean Sea). *Continental Shelf Research*, 149 (October 2016), 151-161.

Frassetto, R., Backus, R.H., Hays, E., 1962. Sound-scattering layers and their relation to thermal structure in the Strait of Gibraltar. *Deep Sea Research and Oceanographic Abstracts*, 9 (72), 69-72.

García-Gómez, C., Yebra, L., Cortés, D., Sánchez, A., Alonso, A. *et al.,* 2020. Shifts in the protist community associated to an anticyclonic gyre in the Alboran Sea (Mediterranean Sea). *FEMS microbiology ecology*, 93 (11).

García, C.M., Jimenez-Gomez, F., Rodríguez, J., Bautista, B., Estrada, M. *et al.,* 1994. The size structure and functional composition of ultraplankton and nanoplankton at a frontal station in the Alboran Sea. Working groups 2 and 3 Report. *Scientia Marina*, 58 (1-2), 43-52.

García Lafuente, J., Delgado, J., Vargas, J.M., Vargas, M., Plaza, F. *et al.,* 2002. Low-frequency variability of the exchanged flows through the Strait of Gibraltar during CANIGO. *Deep-Sea Research Part II: Topical Studies in Oceanography*, 49 (19), 4051-4067.

Garwood, B.J.C., Musgrave, R.C., Lucas, A.J., 2020. Life in Internal Waves. *Oceanography*, 33 (3).

Gómez-Jakobsen, F.J., Mercado, J.M., Cortés, D., Yebra, L., Salles, S., 2019. A first description of the summer upwelling off the Bay of Algeciras and its role in the northwestern Alboran Sea. *Estuarine, Coastal and Shelf Science*, 225 (May), 106230.

Gómez, F., Echevarría, F., García, C.M., Prieto, L., Ruiz, J. *et al.,* 2000. Microplankton distribution in the strait of Gibraltar: coupling between organisms and hydrodynamic structures. *Journal of Plankton Research*, 22 (4), 603-617.

Gómez, F., Gorsky, G., García-Górriz, E., Picheral, M., 2004. Control of the phytoplankton distribution in the Strait of Gibraltar by wind and fortnightly tides. *Estuarine, Coastal and Shelf Science*, 59 (3), 485-497.

González-García, C., Forja, J., González-Cabrera, M.C., Jiménez, M.P., Lubián, L.M., 2018. Annual variations of total and fractionated chlorophyll and phytoplankton groups in the Gulf of Cadiz. *Science of The Total Environment*, 613, 1551-1565.

Gorsky, G., Ohman, M.D., Picheral, M., Gasparini, S., Stemmann, L. *et al.,* 2010. Digital zooplankton image analysis using the ZooScan integrated system. *Journal of Plankton Research*, 32 (3), 285-303.

Grasshoff, K., Ehrhardt, M., Kremling, K., 1983. Methods of Seawater Analysis.2nd ed. Verlag Chemie, Weinheim, Germany.

Van Haren, H., 2014. Internal wave-zooplankton interactions in the Alboran Sea (W-Mediterranean). *Journal of Plankton Research*, 36 (4), 1124-1134.

Herman, A.W., 2009. LOPC Data Analyses – Standard LOPC. Retrieved from http://www.alexherman.com/lopc_post.php.

Herman, A.W., Beanlands, B., Phillips, E.F., 2004. The next generation of Optical Plankton Counter: the Laser-OPC. *Journal of Plankton Research*, 26 (10), 1135-1145.

Holm-Hansen, O., Hewes, C. D. 2004. Deep chlorophyll-a maxima (DCMs) in Antarctic waters. *Polar Biology*, 27 (11), 699-710.

Hu, Q., Davis, C., 2006. Accurate automatic quantification of taxa-specific plankton abundance using dual classification with correction Qiao. *Marine Ecology Progress Series*, 306, 51-61.

Izquierdo, A., Mikolajewicz, U., 2019. The role of tides in the spreading of Mediterranean Outflow waters along the southwestern Iberian margin. *Ocean Modelling*, 133, 27-43.

Jackson, G.A., Checkley, D.M., 2011. Particle size distributions in the upper 100m water column and their implications for animal feeding in the plankton. *Deep Sea Research Part I: Oceanographic Research Papers,* 58 (3), 283-297.

Kelley, D., Richards, C., 2016. oce: Analysis of Oceanographic Data. Retrieved from https://cran.r-project.org/package=oce.

Kolbowski, J., Schreiber, U., 1995. Computer-Controlled Phytoplankton Analyzer Based on a 4-Wavelengths Pam Chlorophyll Fluorometer. In'Photosynthesis: From Light to Biosphere'. (Ed. P Mathis) pp. 825-828.

León, P., Blanco, J.M., Flexas, M.M., Gomis, D., Reul, A. *et al.* 2015. Surface mesoscale pico-nanoplankton patterns at the main fronts of the Alboran Sea. *Journal of Marine Systems*, 143, 7-23.

Llope, M., de Carvalho-Souza, G.F., Baldó, F., González-Cabrera, C., Jiménez, M.P. *et al.,* 2020. Gulf of Cadiz zooplankton: Community structure, zonation and temporal variation. *Progress in Oceanography*, 186 (June), 102379.

Lund, J.W.G., Kipling, C., Le Cren, E.D., 1958. The Inverted Microscope Method of Estimating Algal Numbers and the Statistical Basis of Estimations by Counting. *Hydrobiologia*, 11 (2), 143-170.

Macías, D., García, C.M., Echevarría, F., Vázquez-Escobar, Á., Bruno, M., 2006. Tidal induced variability of mixing processes on Camarinal Sill (Strait of Gibraltar): A pulsating event. *Journal of Marine Systems*, 60 (1-2), 177-192.

Macías, D., Martin, A.P., García Lafuente, J., García, C.M., Yool, A. *et al.,* 2007a. Analysis of mixing and biogeochemical effects induced by tides on the Atlantic-Mediterranean flow in the Strait of Gibraltar through a physical-biological coupled model. *Progress In Oceanography*, 74 (2-3), 252-272.

Macías, D., Navarro, G., Echevarría, F., García, C.M., Cueto, J.L., 2007b. Phytoplankton pigment distribution in the northwestern Alboran Sea and meteorological forcing: A remote sensing study. *Journal of Marine Research*, 65, 523-543.

Macías, D., Bruno, M., Echevarría, F., Vázquez-Escobar, Á., García, C.M., 2008a. Meteorologically-induced mesoscale variability of the North-western Alboran Sea (southern Spain) and related biological patterns. *Estuarine, Coastal and Shelf Science*, 78 (2), 250-266.

Macías, D., Lubián, L.M., Echevarría, F., Huertas, I.E., García, C.M., 2008b. Chlorophyll maxima and water mass interfaces: Tidally induced dynamics in the Strait of Gibraltar. *Deep-Sea Research I*, 55 (7), 832-846.

Macías, D., Somavilla, R., González-Gordillo, J. I., Echevarría, F., 2010. Physical control of zooplankton distribution at the Strait of Gibraltar during an episode of internal wave generation. *Marine Ecology Progress Series*, 408, 79-85.

Macías, D., Rodríguez-Santana, Á., Ramírez-Romero, E., Bruno, M., Pelegrí, J.L. *et al.,* 2013. Turbulence as a driver for vertical plankton distribution in the subsurface upper ocean. *Scientia Marina*, 77, 541-549.

Macpherson, E., Gordoa, A., 1996. Biomass spectra in benthic fish assemblages in the Benguela system. *Marine Ecology Progress Series*, 138 (1-3), 27-32.

Margalef, R., 1978. Life-forms of phytoplankton as survival alternatives in an unstable environment. *Oceanologica Acta*, 1 (4), 493-509.

Mercado, J.M., Cortés, D., Ramírez, T., Gómez, F., 2012. Decadal weakening of the wind-induced upwelling reduces the impact of nutrient pollution in the Bay of Málaga (western Mediterranean Sea). *Hydrobiologia*, 680 (1), 91-107.

Mercado, J.M., Gómez-Jakobsen, F., Cortés, D., Yebra, L., Salles, S. *et al.,* 2016. A method based on satellite imagery to identify spatial units for eutrophication management. *Remote Sensing of Environment*, 186, 123-134.

Mercado, J.M., Ramírez, T., Cortés, D., Sebastián, M., Vargas-Yáñez, M., 2005. Seasonal and inter-annual variability of the phytoplankton communities in an upwelling area of the Alborán Sea (SW Mediterranean Sea). *Scientia Marina*, 69 (3), 451-465.

Montagnes, D.J.S., Berges, J.A., Harrison, P.J., Taylor, F.J.R., 1994. Estimating carbon, nitrogen, protein, and chlorophyll a from volume in marine phytoplankton. *Limnology and Oceanography*, 39 (5), 1044-1060.

Morillo-García, S., Valcárcel-Pérez, N., Cózar, A., Ortega, M.J., Macías, D. *et al.,* 2014. Potential Polyunsaturated Aldehydes in the Strait of Gibraltar under Two Tidal Regimes. *Marine drugs*, 12 (3), 1438-59.

Navarro, G., Ruiz, J., 2006. Spatial and temporal variability of phytoplankton in the Gulf of Cádiz through remote sensing images. *Deep Sea Research II*, 53 (11-13), 1241-1260.

Picheral, M., Colin, S., Irisson, J.O., 2017. EcoTaxa, a tool for the taxonomic classification of images. Retrieved from http://ecotaxa.obs-vlfr.fr.

Platt, T., Denman, K., 1978. The structure of pleagic marine ecosystems. *Rapports et procès-verbaux des réunions*, 173, 60-65.

Prieto, L., García, C.M., Corzo, A., Ruiz, J., Echevarría, F., 1999. Phytoplankton , bacterioplankton and nitrate reductase activity distribution in relation to physical structure in the northern Alborán Sea and Gulf of Cadiz (southern Iberian Peninsula). *Boletín-Instituto Español de Oceanografía,* 15 (1/4), 401-412.

Prieto, L., Navarro, G., Rodríguez-Gálvez, S., Huertas, I.E., Naranjo, J.M. *et al.,* 2009. Oceanographic and meteorological forcing of the pelagic ecosystem on the Gulf of Cadiz shelf (SW Iberian Peninsula). *Continental Shelf Research*, 29 (17), 2122-2137.

R Core Team. 2008. R: A language and environment for statistical computing. R Foundation for Statistical Computing. Retrieved from http://www.r-project.org.

Ramírez-Romero, E., Macías, D., García, C.M., Bruno, M., 2014. Biogeochemical patterns in the Atlantic Inflow through the Strait of Gibraltar. *Deep-Sea Research Part I: Oceanographic Research Papers*, 85, 88-100.

Razouls, C., de Bovée, F., Kouwenberg, J.H.M., Desreumaux, N., 2005. Diversity and Geographic Distribution of Marine Planktonic Copepods. Retrieved from http://copepodes.obs-banyuls.fr/en.

Reul, A., Jimenez-Gomez, F., Blanco, J.M., Bautista, B., Sarhan, T. *et al.,* 2005. Variability in the spatio-temporal distribution and size-structure of phytoplankton across an upwelling area in the NW-Alboran Sea, (W-Mediterranean). *Continental Shelf Research*, 25 (5-6), 589-608.

Reul, A., Vargas-Yáñez, M., Jimenez-Gomez, F., Echevarría, F., García Lafuente, J. *et al.* 2002. Exchange of planktonic biomass through the Strait of Gibraltar in late summer conditions. *Deep Sea Research II*, 49, 4131-4144.

Rodríguez, J., Blanco, J.M., Jiménez-Gómez, F., Echevarría, F., Gil, J. *et al.,* 1998. Patterns in the size structure of the phytoplankton community in the deep fluorescence maximum of the Alboran Sea (southwestern Mediterranean). *Deep-Sea Research Part I: Oceanographic Research Papers*, 45 (10), 1577-1593.

Roselli, L., Basset, A., 2015. Decoding size distribution patterns in marine and transitional water phytoplankton: From community to species level. *PLoS ONE*, 10 (5), 1-21.

Sabetta, L., Basset, A., Spezie, G., 2008. Marine phytoplankton size-frequency distributions: Spatial patterns and decoding mechanisms. *Estuarine, Coastal and Shelf Science*, 80 (1), 181-192.

Sala, I., 2021. Physical-biological interaction in the Strait of Gibraltar: The Trafalgar-Alborán connection. PhD Thesis. Universidad de Cádiz. Cádiz (Spain).

Sala, I., Navarro, G., Bolado-Penagos, M., Echevarría, F., García, C.M., 2018. High-chlorophyll-area assessment based on remote sensing observations: The case study of Cape Trafalgar. *Remote Sensing*, 10 (2), 165.

Sampaio De Souza, C., Mafalda Jr, P., Salles, S., Ramírez, T., Cortés, D. *et al.*, 2011. Seasonal Changes in the Distribution and Abundance of Marine Cladocerans of the Northwest Alboran Sea (Western. *Brazilian archives of biology an technology*, 54 (June), 543-550.

Sarhan, T., Vargas-Yáñez, M., 2000. Upwelling mechanisms in the northwestern Alboran Sea. *Journal of Marine Systems*, 23, 317-331.

Sheldon, R.W., Prakash, A., Sutcliffe Jr,W., 1972. The size distribution of particles in the ocean 1. *Limnology and oceanography*, 17 (3), 327-340.

Sieracki, C., Sieracki, M.E., Yentsch, C., 1998. An imaging-in-flow system for automated analysis of marine microplankton. *Marine Ecology Progress Series*, 168, 285-296.

Vargas-Yáñez, M., Viola, T. S., Jorge, F. P. F. P., Rubín, J. P., and Garcia-Martinez, M. C. 2002. The influence of tide-topography interaction on low-frequency heat and nutrient fluxes . Application to Cape Trafalgar. *Continental Shelf Research*, 22, 115-139.

Vázquez-Escobar, Á., Flecha, S., Bruno, M., Macías, D., Navarro, G., 2009. Internal waves and short-scale distribution patterns of chlorophyll in the Strait of Gibraltar and Alborán Sea. *Geophysical Research Letters*, 36 (23), 1-6.

Verity, P.G., Robertson, C.Y., Tronzo, C.R., Andrews, M.G., Nelson, J.R. *et al.,* 1992. Relationships between cell volume and the carbon and nitrogen content of marine photosynthetic nanoplankton. *Limnology and Oceanography*, 37 (7), 1434-1446.

Vives, F., Santamaría, G., Trepat, I., 1975. El zooplancton de los alrededores del estrecho de Gibraltar en junio-julio de 1972. *Resultados Expediciones Científicas del Buque Oceanográfico "Cornide de Saavedra"* 4, 7-100.

WoRMS Editorial Board. 2021. World Register of Marine Species. doi: 10.14284/170.

Yebra, L., Herrera, I., Mercado, J. M., Cortés, D., Gómez-jakobsen, F. *et al.,* 2018. Zooplankton production and carbon export fl ux in the western Alboran Sea gyre (SW Mediterranean) Málaga Coast. 167 (July), 64-77.

Yebra, L., Putzeys, S., Cortés, D., Mercado, J.M., Gómez-Jakobsen, F. *et al.*, 2017. Trophic conditions govern summer zooplankton production variability along the SE Spanish coast (SW Mediterranean). *Estuarine, Coastal and Shelf Science*, 187, 134-145.

Yentsch, C.S., Menzel, D.W., 1963. A method for the determination of phytoplankton chlorophyll and phaeophytin by fluorescence. *Deep-Sea Research*, 10, 221-231.

Zheng, H., Wang, R., Yu, Z., Wang, N., Gu, Z. *et al.,* 2017. Automatic plankton image classification combining multiple view features via multiple kernel learning. *BMC Bioinformatics*, 18 (238), 1-18.

Zhou, M., 2006. What determines the slope of a plankton biomass spectrum? *Journal of Plankton Research*, 28 (5), 437-448.

Supplementary Data

The following supplementary information is available online for the article:

Fig. S1: Average values of physical and biogeochemical variables defining each cluster during spring and neap tides. Purple bars represent CL1, green bars for CL2.

Fig. S2: Picoplankton groups biomass distribution. *Synechococcus* (A-B), *Prochlorococcus* (C-D) and Cryptophytes (E-F) biomass (mgC m^{-3}) during spring (A, C, E) and neap tides (B, D, F).

Fig. S3: Main microplankton groups biomass (mgC m^{-3}) distribution during spring (A, C, E, G) and neap (B, D, F, H) tides. A and B represent diatoms, C and D dinoflagellates, E and F correspond to tintinnids, and G and F for silicoflagellates. Note different scales among groups.

Fig. S4: Mean temperature, (A) and N2 (B) profiles averaged for all the stations. The dashed lines represent the 20th and 80th percentiles in both plots.

Table S1. Average values of physical and biogeochemical parameters defining each cluster during spring and neap tides. Mean, N, standard deviation (SD) and range.

Table S2. Main pico and nanoplankton groups cell densities (cell mL^{-1}) and biomass.

Table S3. Microplankton abundance (cell mL^{-1}) and biomass (mgC m^{-3}) by major groups during neap and spring tides.

Table S4. Mesoplankton abundance (ind m-3) and biomass (mgC m^{-3}) by major groups during neap and spring tides.

Table S5. Summary scheme signing main features defining each cluster.

Table S6. Total abundance of copepods orders (ind m^{-3}).

Table S5. Summary scheme signing main features defining each cluster.

Table S6. Total abundance of copepods orders (ind m^{-3}).